

# TEMPLATE-ASSISTED FABRICATION AND DIELECTROPHORETIC MANIPULATION OF PZT MICROTUBES

VLADIMÍR KOVAL

*Institute of Materials Research SAS, Watsonova 47, 043 53 Košice, Slovak Republic*

E-mail: vkoval@imr.saske.sk

Submitted January 10, 2012; accepted June 25, 2012

**Keywords:** PZT, Microtubes, Vacuum infiltration, Dielectrophoresis

*Mesoscopic high aspect ratio ferroelectric tube structures of a diverse range of compositions with tailored physical properties can be used as key components in miniaturized flexible electronics, nano- and micro-electro-mechanical systems, nonvolatile FeRAM memories, and tunable photonic applications. They are usually produced through advanced “bottom-up” or “top-down” fabrication techniques. In this study, a template wetting approach is employed for fabrication of  $\text{Pb}(\text{Zr}_{0.52}\text{Ti}_{0.48})\text{O}_3$  (PZT) microtubes. The method is based on repeated infiltration of precursor solution into macroporous silicon (Si) templates at a sub-atmospheric pressure. Prior to crystallization at 750°C, free-standing tubes of a 2- $\mu\text{m}$  outer diameter, extending to over 30  $\mu\text{m}$  in length were released from the Si template using a selective isotropic-pulsed  $\text{XeF}_2$  reactive ion etching. To facilitate rapid electrical characterization and enable future integration process, directed positioning and aligning of the PZT tubes was performed by dielectrophoresis. The electric field-assisted technique involves an alternating electric voltage that is applied through pre-patterned microelectrodes to a colloidal suspension of PZT tubes dispersed in isopropyl alcohol. The most efficient biasing for the assembly of tubes across the electrode gap of 12  $\mu\text{m}$  was a square wave signal of 5  $V_{\text{rms}}$  and 10 Hz. By varying the applied frequency in between 1 and 10 Hz, an enhancement in tube alignment was obtained.*

## INTRODUCTION

Shrinking electronic device size to micro- and nano-scale dimensions leads material scientists and engineers to a desire to use one-dimensional (1-D) structures, such as tubes, wires or rods for manipulating nanoobjects with nanotools, handling terabyte of information in nonvolatile memories, sensing forces at piconewton scales, and inducing gigahertz motion. Arrays of high aspect ratio ferro- and piezoelectric tube structures are anticipated to offer advantages in a variety of technologically possible device applications, including miniaturized piezoelectric sensors and actuators, pyroelectric detectors, fluidic delivery systems, trenched DRAM memory capacitors, and tunable photonic devices due to their small size, increased electro-active surface area and unique properties when compared to their bulk counterparts. [1, 2, 3, 4, 5]

In the last decade, a numerous new chemical synthesis methods and advanced “bottom-up” and “top-down” fabrication techniques has been developed for producing 1-D tube structures. [6, 7] Among others, a template-assisted wetting method is referred to as most versatile and effective technique that allows the size, shape and structural properties of tubes to be easily controlled by the template used. [8] Luo *et al.*

[9] prepared an ordered array of hundreds ferroelectric nanotubes by using silicon templates with a regular periodic array of pores. Bharadwaja *et al.* [10] improved the mold replication technique by reducing the pressure above liquid precursor to facilitate uniform coating the inside of the pores during the wetting process. They also demonstrated that the phase purity of the PZT tubes can be increased by releasing the tubes from the Si template before annealing, which prevents the reaction between the PZT and silicon at elevated crystallization temperatures. More recently, a highly ordered array of ultra-thin-walled PZT nanotubes were synthesized in a porous alumina membrane through sol-gel synthesis combined with a spin-coating technique. [11] Mist-deposition template derived high aspect ratio ferroelectric structures made of PZT were also reported in the literature. [12] Ferroelectricity and piezoelectricity were confirmed to exist in both the PZT microtubes and PZT nanotubes of several tens to several hundreds nanometers wall thickness. [9, 10, 11, 12]

The as-synthesized ferroelectric tube structures of a small size can serve directly as functional elements of miniaturized devices. For the realization of simple planar geometries or complex 3-D device designs with reliable electrical connections, the development of an appropriate method is required to position and align

large quantities of discrete ferroelectrics as controllable building blocks. Some useful and efficient approaches have been proposed for organic particles and inorganic wires and tubes, wherein chemical surface treatment, magnetic field, or an electric field is utilized for manipulation of micron sized and nanometer objects. [13] However, a selective and controllable assembly of ferroelectric 1-D like structures with high aspect ratio has not been reported yet. One of the most promising candidates is dielectrophoresis, which uses an electric field. Unlike electrophoresis, which is related to the migration of charged particles toward the electrode of opposite charge, dielectrophoresis is a translational motion of neutral particles to regions of higher field strength caused by the polarization of the particles in an external non-uniform electric field. The fundamentals of dielectrophoresis were introduced by Pohl in 1951. [14] Since the feasibility of dielectrophoretic manipulation of particles with typical sizes down to the micro- and nanorange was demonstrated by using microstructured electrodes to collect protein molecules [15], a number of applications has been found for the technique. These include assembling conductive and semiconducting carbon nanotubes, CdS and GaN nanowires, ZnO nanostructures, gold nanoparticles and wires. [16, 17, 18, 19, 20] In case of ferroelectric tube structures, the dielectrophoretic technique would provide technologists and nanoscientists with some benefits and advantages for batch manufacturing of the next generation micro-electro-mechanical system (MEMS) and N(ano)EMS devices. Besides the technique is compatible with conventional top-down Si micro- and nanomachining techniques and allows for integration upon arbitrary substrates including those that require low temperature processing (e.g., flexible substrates), the electrode array used for directed assembly can serve as a functional electrical connection in hierarchical device structures. Another benefit is that the position and number density of assembled ferroelectrics can be easily controlled by the adjusting the electric field.

A theoretical formulation of the dielectrophoretic force, as introduced by Jones [21], reveals that the force experienced by the manipulated object depends on a number of parameters, such as the arrangement of the electrodes - electrode shape, gap size and numbers; the amplitude and frequency of the electric field, the field application time and the resulting electric field distribution. By changing these factors, the electric-field induced movement of small sized objects in surrounding medium can be controlled. Whether the force on the manipulated object is positive (attracting) or negative (repelling) is determined by the polarizability factor, often called as the Clausius-Mossotti factor, whose value mainly depends on the dielectric properties of both the manipulated object and the surrounding medium.

In this paper, a simple and effective wafer-scale technique is used for the fabrication of ferroelectric

microtubes. The method is based on repeated immersion of a macroporous silicon template into a liquid PZT precursor under a sub-atmospheric pressure. Upon 20 consecutive vacuum infiltrations, tubes with an outer diameter of 2  $\mu\text{m}$ , length of about 30  $\mu\text{m}$  and wall thickness of 400 nm were achieved. The X-ray diffraction analysis and scanning electron microscopy were employed to confirm a formation of the perovskite phase and hollow structure of the crystallized PZT tubes. The as-synthesized microtubes were assembled, in the next step, from solution onto pre-patterned electrodes using AC dielectrophoresis. A promising aspect of this research is the possibility to quickly and simply create electrical connections to ferroelectric microtubes at ambient conditions, and thereby it allows for making an electrical testing structure for potential applications in high-storage memory capacitors and high-performance piezoelectric actuators and sensors. We examine and discuss the influence of a number of dielectrophoretic parameters in details and summarize that careful electrode design and low-frequency low-amplitude square wave signals will allow for arranging high aspect ratio ferroelectric microtube structures at designed positions on silicon wafers.

## EXPERIMENTAL

The 30- $\mu\text{m}$  long PZT microtubes with wall thickness of 400 nm and aspect ratio as high as 20 were prepared using a template-assisted mold replication technique that integrates a sol-gel process with vacuum promoted wetting of the pore wall of porous templates by liquid precursor. Silicon templates with an ordered array of pores were processed by deep reactive-ion etching and obtained from Nordoca Inc., Edmonton, Canada. The as-received templates were pre-cleaned in an oxygen plasma etcher (Plasma Technology Inc., Concord, MA) followed by chemical etching in 10:1 buffered oxide etch solution (BOE, J. T. Baker). The PZT precursor of a nominal stoichiometric composition  $\text{Pb}_{1.2}(\text{Zr}_{0.52}\text{Ti}_{0.48})\text{O}_3$  was prepared by sol-gel method, as described elsewhere. [22]

A schematic for the process of fabrication of PZT microtubes is shown in Figure 1. At the beginning the cleaned and dried silicon template was immersed in an evacuated container of PZT solution for about 5 min. This makes the sol precursor infiltrate uniformly into the pores with the help of pressure balancing. As a result, a layer of the PZT is formed on the pore walls. Then the Si template with the PZT layer coated pore walls was taken out and the excess sol on its surface was wiped off using a cotton swab dipped in 2-methoxyethanol. In the next step the template was heated from room temperature to 300-350°C in air. The PZT layer on the sidewalls of the pores was transformed into an amorphous oxide layer by annealing at the above temperatures for 3 min. In order

to obtain the microtubes with desired wall thickness, the “infiltration-pyrolysis” process was repeated several times. Typically, a 400-nm-wall thickness was achieved in 20 successive infiltrations. Since a chemical reaction between the Si and the PZT is detrimental to perovskite phase formation in PZT, the pyrolyzed tubes were released from the template along the majority of their length by selective etching of silicon.

Approximately 30  $\mu\text{m}$  of silicon was removed in 30 min using an isotropic-pulsed  $\text{XeF}_2$  reactive ion etching tool (RIE, Xetch e-series, Xactix Inc., Pittsburgh, PA). Finally, an ordered array of free-standing PZT microtubes, anchored at the bottom of the template, was obtained by fast annealing in 99.98 % oxygen at a temperature of 750°C for 2 min (a rapid thermal annealer, model Tsunami series RTP-600S). The microstructure and morphology of microtubes were investigated by scanning electron microscope (SEM, model Hitach S-3500N, Pleasanton, CA). Structural characterization on the tubes was carried out via X-ray diffraction (XRD, Scintag, Sunnyvale, CA) using  $\text{CuK}\alpha$  radiation for  $2\theta$  angular scans ranging from 20° to 60° with a 0.025° step size.

For assembly experiments, microtubes were released completely from the template by rinsing in iso-

propanol (IPA) and subsequently suspended into IPA filled container by sonification for 5 s. The solution was then pipetted onto a pre-patterned silicon wafer. The interdigitated electrodes (Ti/Au = 10/60 nm, Figure 2) were processed using electron-beam lithography followed by metal deposition and a standard lift-off procedure. Four different electrode array structures with electrodes gap sizes of 6  $\mu\text{m}$ , 9  $\mu\text{m}$ , 12  $\mu\text{m}$  and 15  $\mu\text{m}$ , respectively, were used in our experiments. An HP33120A (Hewlett-Packard, Palo Alto, CA) function generator was connected to a voltage amplifier (790 series, AVC Instrumentation) to generate sufficiently large ac electric fields between the electrodes. The sinusoidal and square-wave signals ranging from 1 to 15  $\text{V}_{\text{rms}}$  were applied at frequencies between 1 Hz and 1 MHz across the microtubes suspension through the two gold microprobes. An optical microscope equipped with a CCD camera was used to observe and capture an image of the tubes after manipulation.

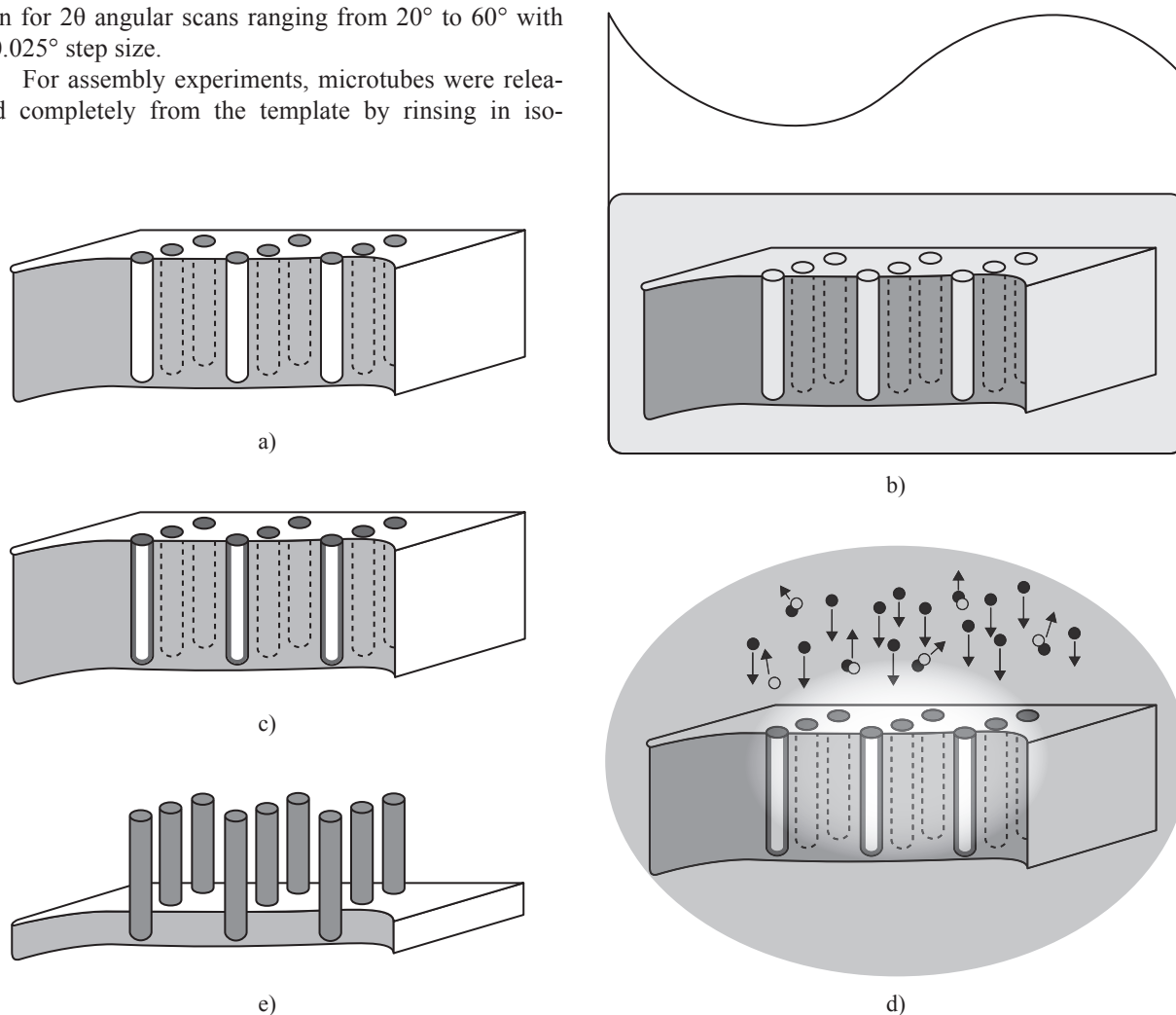
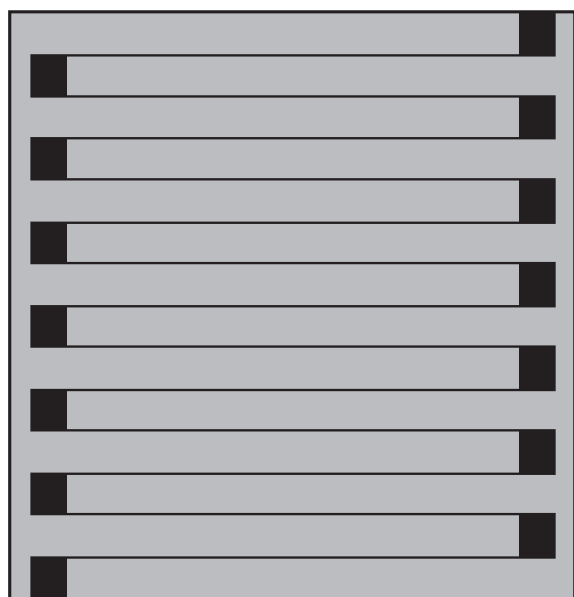
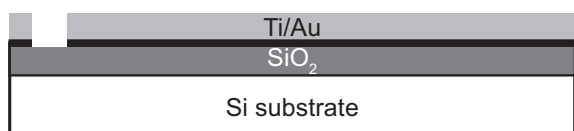


Figure 1. Fabrication of PZT microtubes using vacuum infiltration method: a) a pre-cleaned macroporous silicon template, b) immersing the template into PZT solution under vacuum, c) a layer of PZT formed on the pore walls after pyrolysis at 350°C/2 min, d)  $\text{XeF}_2$  gas phase etch process to release the tubes, e) free-standing ferroelectric tubes annealed at 750°C/2 min.

RESULTS AND DISCUSSION



a)



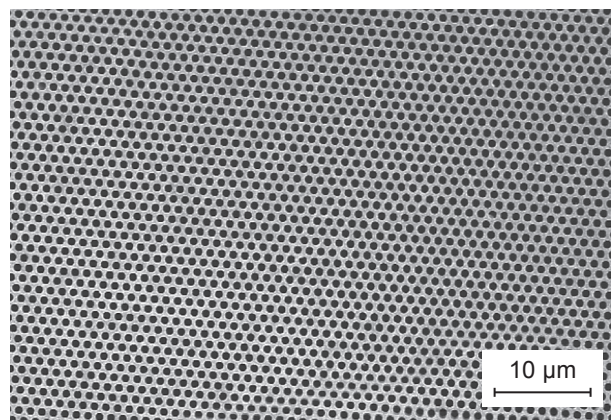
b)



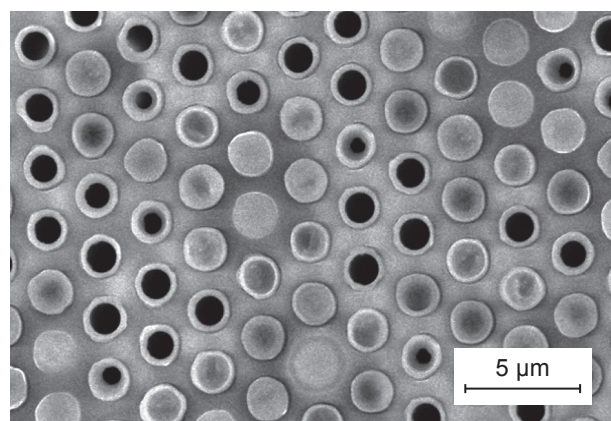
c)

Figure 2. Interdigitated electrode structure: a), b) a schematic diagram – top and side view, c) an optical microscope image – top view.

A SEM micrograph of an unfilled silicon template with a regular hexagonal array of two-dimensional pores with the diameter of 2 μm and the inter-pore distance of 1 μm is shown in Figure 3a. After 20 infiltrations, as seen in Figure 3b, all of the pores have sidewalls covered by a PZT layer. The same sample is shown in a cross-



a)



b)

Figure 3. SEM images of macroporous silicon templates: a) unfilled, b) infiltrated with PZT.

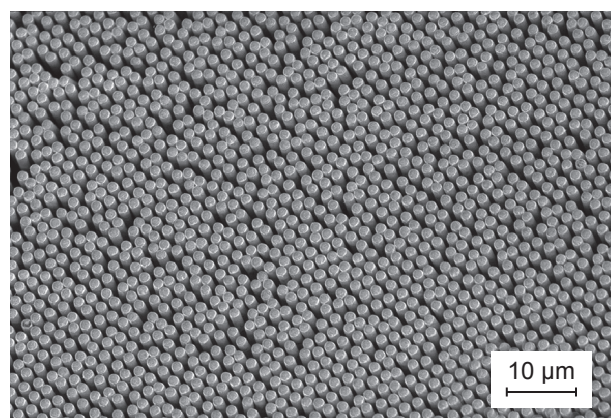
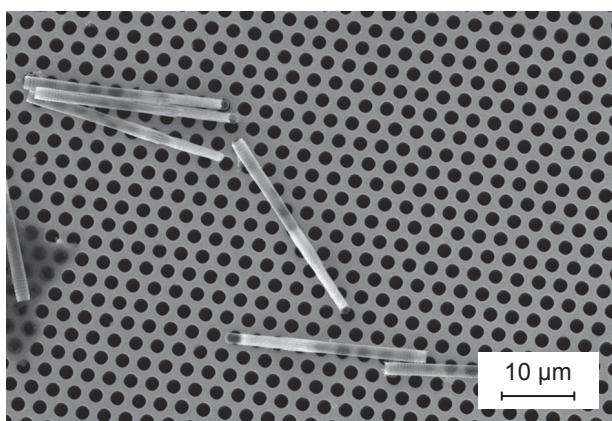


Figure 4. SEM photograph of an ordered array of PZT microtubes.

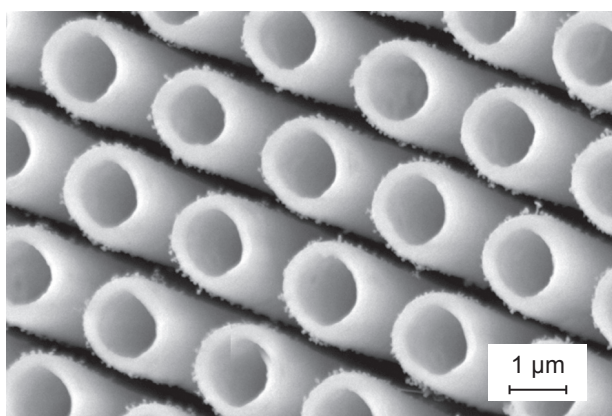
sectional view (Figure 4) after partial removal of the host Si matrix followed by thermal annealing at 750°C for 2 min in oxygen ambient. The result of an isotropic XeF<sub>2</sub> reactive ion etching process is a regular array of free-standing microtubes anchored to the Si template only at the tube base. It is clear that the crystallized tubes are straight, nearly uniform, and completely discrete. It should be noted that the repeated vacuum infiltration allowed the PZT solution to deposit evenly at the bottom of the Si template pores.

In Figure 5, a SEM image shows a bunch of PZT tubes that were released completely from the template by sonification. Their hollow nature is demonstrated in Figure 5b, in which the open ends of individual tubes are depicted. A wall thickness can be estimated from the micrograph to about 400 nm. Because of pore profile irregularities caused natively by deep reactive ion etching of the Si templates, the rippled sidewalls are observed on microtubes close to the open ends.

X-ray diffraction analysis (Figure 6) demonstrates that the partially released PZT microtubes have perovskite phase after crystallization process at 750°C for 2 min in a rapid thermal annealer. The most intense reflection at about  $2\theta = 70^\circ$  and the weak reflection



a)



b)

Figure 5. SEM image of the released tubes (a) and a hollow structure (b).

at 28,5° are due to the Si substrate. In addition to perovskite phase peaks, small Bragg reflections of a pyrochlore phase are noticed in the XRD pattern. Kwok *et al.* [23] and Hamed *et al.* [24] reported that formation of an intermediate pyrochlore or fluorite phase during synthesis of lead-based ferroelectric films on substrates and free-standing PZT films, respectively, is kinetically favored over the perovskite phase. An additional second phase peak occurring at about 36° might be associated with the oxyfluorides of Zr/Ti cations forming in the structure due to XeF<sub>2</sub> gas phase etching of silicon. [10] Bharadwaja *et al.* [12] revealed that the fluoride contamination can be minimized by mild boric acid treatment. As it has been proposed for the template-assisted processing of PbTiO<sub>3</sub> tubes, an extension of annealing time would result in transformation of a metastable fluorite phase into the perovskite phase. [8] In order to investigate the effect of annealing conditions on phase purity of PZT, different thermal budgets were used for crystallization of microtubes in the present work. However, heat treatment experiments at very high temperatures or extended times resulted in an irreversible damage of the tubes. The representative SEM images of broken microtubes are shown in Figure 7. While an annealing at a temperature of 800°C for 1 min caused buckling and melting of tubes (Figure 7a), the prolonged annealing at 750°C for 10 min resulted in their squeezing and joining (Figure 7b).

The results show that the vacuum infiltration technique is a convenient method for producing the high aspect ratio ferroelectric microtube structures with tailored dimensions. Successive infiltrations of macroporous Si templates under sub-atmospheric pressure facilitate uniform, thickness-tunable coating the inside of the Si template pores. On partial removal of the Si template by XeF<sub>2</sub> gas phase treatment, it is possible to produce an ordered array of ceramic microtubes in which each tube is completely discrete. However,

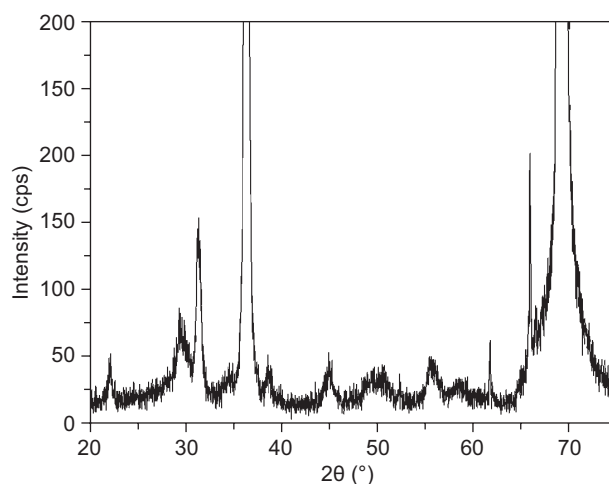
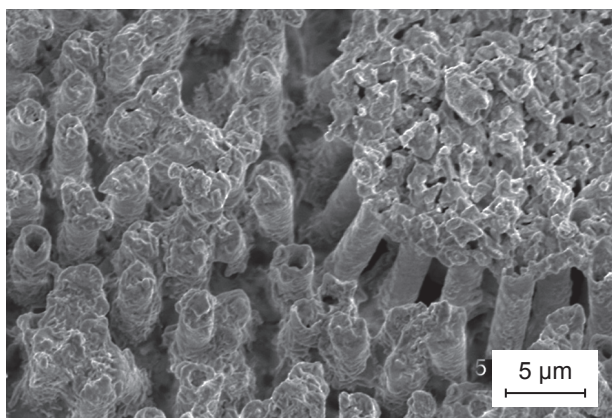
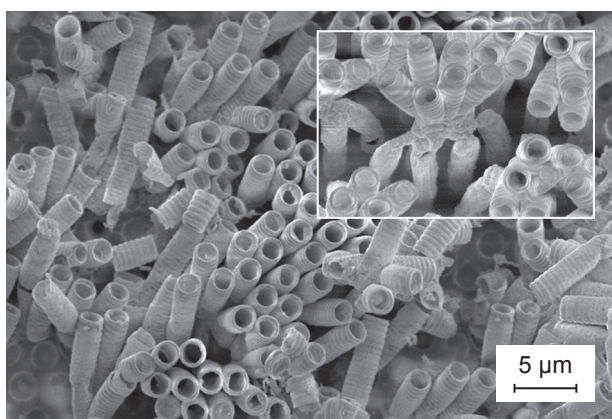


Figure 6. X-ray diffraction pattern of PZT microtubes anchored at the bottom of the Si template.



a)

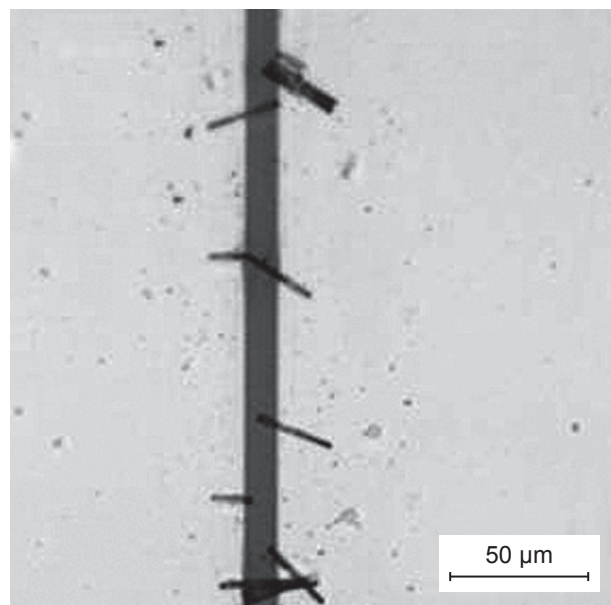


b)

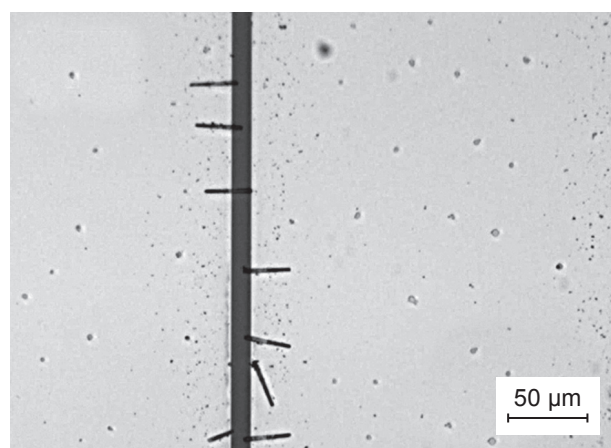
Figure 7. SEM images of broken tubes after annealing: a) at 800°C for 1 min, b) at 750°C for 10 min.

control of the microstructure and phase composition of free-standing PZT microtube structures remains a challenge. The processing conditions related to thermal budget and silicon removal process need to be further optimized.

Discrete microtubes were further manipulated by AC dielectrophoresis to position and align them at designed positions across the microelectrode array structure for fast future electrical characterization. Figures 8a and 8b show the results from an assembly experiment with a RMS ( $V_{rms}$ ) voltage of 5 V (a square wave) driven at a frequency of 10 Hz. Results are shown for a pair of opposing electrodes with a 12  $\mu\text{m}$  spacing. It is clear that the microtubes, which were deposited and oriented randomly between electrodes at the beginning, aligned in a uniform way and oriented preferentially perpendicular to the direction of the electrodes and parallel to each other. They appear to be randomly positioned along the electrode length and are mostly touching one of the two adjacent electrodes. An additional degree of tube alignment was achieved at a fixed voltage of 5  $V_{rms}$  right before the complete evaporation of isopropanol by varying the frequency of square wave between 10 and 1 Hz. Field-induced oscillations of misaligned tubes



a)

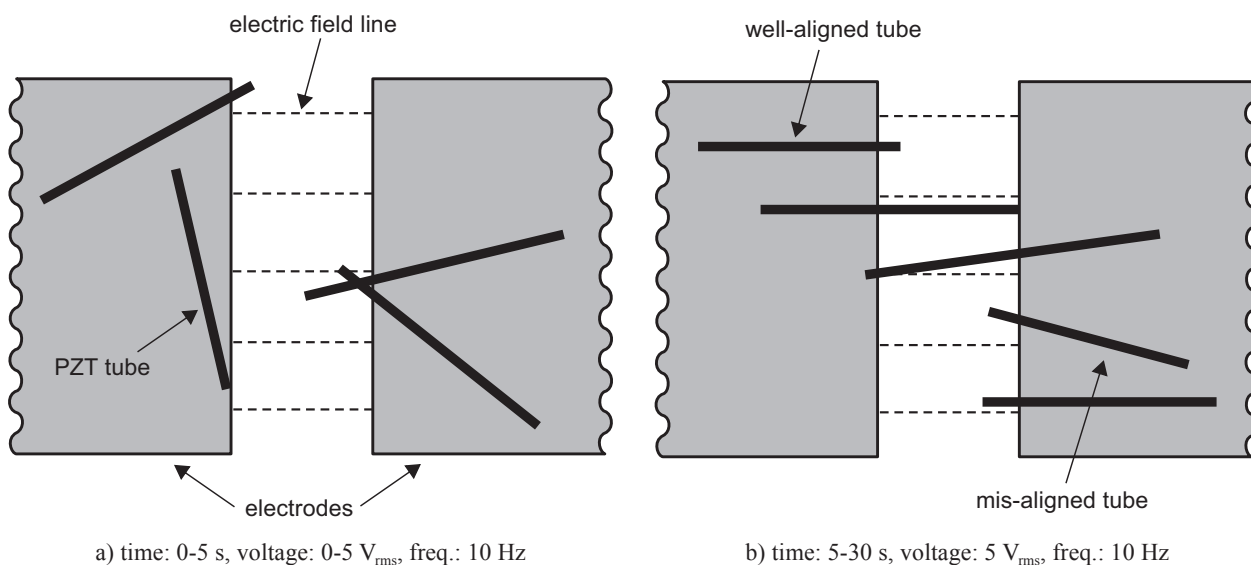


b)

Figure 8. Optical microscope images of the selected area of the electrode array with PZT microtubes assembled between the opposing electrodes with a 12  $\mu\text{m}$  gap by applying a square wave signal of 5  $V_{rms}$  and 10 Hz: a) before, and b) after rapid frequency variation in the range of 1-10 Hz.

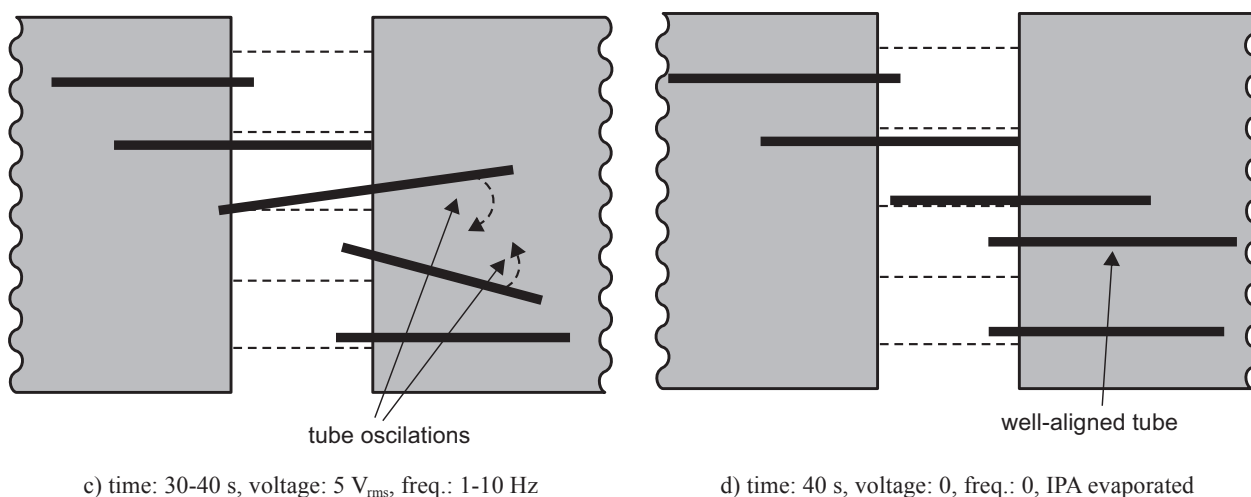
were observed as the frequency was rapidly decreased to 1 Hz. Then, with increasing frequency back to 10 Hz, one end of the tube was suddenly freed, rotated and re-trapped in his new location between the electrodes. We speculate that this effect might be due to the frequency dependent complex polarization factor that causes the changes not only in the dielectrophoretic force but also in the dielectrophoretic torque.

Figure 9 shows an illustration of translation and electrorotation of PZT tubes by dielectrophoresis, including the frequency-variation-induced enhancement in orientation of the tubes. It should be noted that the applied voltage of 3  $V_{rms}$  was not sufficiently large to cause an alignment of tubes. Only a few microtubes



At the beginning of the assembly process, the tubes move randomly. They can be trapped with the same probability at any point of the minima of the electric field occurring between two parallel electrodes because the distribution of the electric field is approximately equal along the electrode gaps.

The dielectrophoretic force acting on a microtube is proportional to the gradient of the electric field. Because the gradient of the electric field drops off quickly with the distance from the electrode, the dielectrophoretic force acts primarily on microtubes that are close to the electrode gaps. As microtubes manipulated by the applied electric field approach the electrode gap, large dielectric force induced by dipole-dipole interaction between the electrodes and tube tips leads to trapping of the tubes between the electrodes. A large fraction of the collected tubes are only in contact with one of the electrodes. They are mostly well aligned in the direction of the electric field.



An enhancement in tube alignment was obtained by varying the frequency of the applied rectangular voltage. Upon the frequency variation between 1 and 10 Hz, misaligned tubes were observed to oscillate at one of the tube tip; while one end of the tube is pivoted, the other end was suddenly freed from its trapped position, rotated and finally re-trapped in a new, energetically more preferable position near the electrode edge with enhanced orientation. By repeating this process several times, the overall alignment of the tubes was improved before the complete evaporation of isopropanol.

PZT microtubes assembled between two parallel rectangular shaped electrodes by dielectrophoresis.

Figure 9. Conceptual illustration of the frequency variation enhanced alignment.

near the centre of the electrode gap exhibited the aligned tendency. On the other side, increasing the electrode voltage from 5 V<sub>rms</sub> to 15 V<sub>rms</sub> at a fixed frequency of 10 Hz resulted in no tubes trapped in the electrode gaps. The tubes drifted away rather than stayed between the electrodes. This can be explained by increased moving speeds,  $v_{DEP} \propto \nabla|E|^2$  [25], at higher electric fields.

The changes in alignment behavior caused by a variation in the amplitude and frequency of the applied square wave signal are due to forces that induce a translational movement and spatial reorientation of PZT microtubes across the microelectrode array structure and can be rationalized by considering the dielectrophoretic force model. [26] The time averaged dielectrophoretic force experienced by microtubes can be approximated through its first dipole moment contribution as [21, 26]

$$\langle \vec{F}_{DEP} \rangle \approx r^2 l \varepsilon_m \operatorname{Re} [\vec{\alpha}] \nabla |\vec{E}_{rms}|^2 \quad (1)$$

where  $r$  is the tube radius,  $l$  is the length of the tube,  $\varepsilon_m$  is the absolute permittivity of the IPA medium,  $\nabla |\vec{E}_{rms}|^2$  is the gradient of the square of the root-mean-square of the electric field and  $\operatorname{Re}[\vec{\alpha}]$  is the real part of the complex effective polarizability or so called the Clausius-Mossotti factor. While the gradient of the field is affected by both the geometry of the electrodes and the applied voltage, the Clausius-Mossotti factor is a function of the dielectric permittivities and conductivities of microtubes and suspending medium, as well as frequency of the applied AC field:

$$\alpha(\omega) = \frac{\varepsilon_t^*(\omega) - \varepsilon_m^*(\omega)}{\varepsilon_m^*(\omega)} \quad (2)$$

where  $\varepsilon^* = \varepsilon - j(\sigma/\omega)$  is the complex permittivity,  $\omega$  is the angular frequency of the applied electric field,  $\sigma$  is the conductivity and  $j$  is the complex number ( $j = \sqrt{-1}$ ). The subscripts  $t$  and  $m$  denote tube and medium, respectively.

The effective dipole moment approximation assumes that only a single dipole is induced on a particle [21]. The particle is assumed to be small compared to the characteristic length of the external electric field, so that the gradient of the electric field is essentially constant in the region surrounding the particle. In addition, it is assumed that the existence of the particle does not disturb its surrounding electric field. For significantly nonuniform electric fields, higher order corrections are needed and multi-pole expansions are necessary. Aubry *et al.* [27] have used Distributed Lagrangian Method and Maxwell Stress Tensor approach to study the dielectrophoretic assembly of rigid spherical particles in an electric field cage. They revealed that it is essential to solve the electric field as a boundary value problem in order to obtain a solution for the dielectrophoretic force on objects with the size comparable to the gap size and captured in the vicinity of microelectrodes. Liu *et al.* [28] studied the range of validity of the dipole moment approximation and compared its accuracy with that of the Maxwell stress tensor calculation. They found that when

the characteristic length of the electric field is larger than twice the diameter of the spherical particles, the dipole moment approximation estimates the dielectrophoretic force in the direction that is perpendicular to the electrode edges with the relative error within 3%. As the characteristic length of the electric field is increased, the accuracy of the dipole moment approximation improves. When the ratio of the particle length and the length scale of the electric field is small, the presence of the particle introduces only a small disturbance in the electric field and the dipole moment approximation provides an excellent approximation.

Following an Equation 1, the dielectrophoretic force is proportional to the gradient of electric field,  $F_{DEP} \propto \nabla E^2$ . This means the higher the voltages at a fixed frequency and the same electrode gaps are, the larger the gradients of the electric field intensity and the greater the forces. In this experiment, the force experienced by microtubes at voltages below 5 V<sub>rms</sub> was not enough to overcome the resistance forces (e.g., gravity, Brownian motion, viscous drag forces) in the solution. A majority of the tubes is loosely pulled and distributed randomly over the electrode array. Although, the tubes dispersed close to the electrodes were attracted to and seated in the electrode gaps by the applied 3-V<sub>rms</sub>-square-wave signal. This can be explained by the fact that the gradient of the electric field drops off quickly with distance from the electrode. With increasing the electrode voltage up to 5 V<sub>rms</sub>, tubes are trapped between the interdigitated electrodes with improved alignment. The effect of the field is anticipated, because the dielectrophoretic force increases with the squared values of the field intensity and gradient, and the movement can proceed only when the effective force of long-range dielectrophoretic attraction between the tubes and electrodes becomes stronger than the Brownian motion or gravity. The force is directed along the gradient of electric field intensity, which is not necessarily aligned with the applied electric field. Raychaudhuri *at al.* [29] revealed that at low frequencies semiconductor nanowires followed the electric field lines back to one of the two opposing electrodes, whereas at higher frequencies the wires were found to move in the direction of the electric field gradient resulting in bridging of nanowires the electrode gap. Our results for ferroelectric PZT microtubes, which are observed only in contact with one of the biased microelectrodes, are consistent with those referred for the low frequency data in References 28 and 29.

The real part of the Clausius-Mossotti factor (Equation 2) gives the frequency dependence and the direction of the dielectrophoretic force. In the low and high frequency limits, the  $\operatorname{Re}[\alpha(\omega)]$  can be simplified as [30]

$$\operatorname{Re}[\alpha(\omega)] = \begin{cases} \frac{\sigma_t - \sigma_m}{\sigma_m}, & \omega \rightarrow 0 \\ \frac{\varepsilon_t - \varepsilon_m}{\varepsilon_m}, & \omega \rightarrow \infty \end{cases} \quad (3)$$

When the conductivity and permittivity of surrounding medium, each dominating in the Hz-kHz and MHz-GHz range, respectively, exceeds that of the manipulated object, negative dielectrophoresis occurs. The objects are then directed away from regions of high field intensities. Otherwise, positive forces lead to attraction. IPA has a high conductivity compared to the ferroelectric microtubes with much higher dielectric permittivity [12], and thus the PZT microtubes are expected to experience the negative dielectrophoresis in the low frequency region. Figure 8a shows that a majority of tubes is collected in the electrode gap, i.e. between opposing electrodes at a frequency of 10 Hz. This demonstrates the negative dielectrophoretic force with negative values of the effective polarizability factor that pushes tubes to regions corresponding to electric field intensity minima. Crews *et al.* [31] identified numerically these low-field points exactly in the center between the two planar plate-like electrodes.

Inspection of the SEM image in Figure 8a reveals that aligned orientation induced by the  $5 V_{\text{rms}} / 10$  Hz square wave signal is somewhat random and even crossed in some regions. Liu *et al.* [28] proposed that thermal fluctuation could randomize an orientation of a microtube oriented along the electric field with one end fixed and the length floating. Another factor that could influence the orientation of PZT tubes is a surface tension [32], an unevenness in the distribution of the strength of the dielectrophoretic force [33], or a variation in dielectrophoretic torque [34]. In general, the torque ( $T_{\text{DEP}}$ ) occurs in dielectrophoretic system when the electric field has a nonuniform phase, which means that there is a rotational component to the field. Since the direction of the effective dipole lags behind the turning field vector by a phase factor associated with the complex, frequency-dependent Clausius-Mossotti factor, dielectrophoretic torque applies on the tube and depends on the out-of-phase component of the dipole. [34] Y. Liu *et al.* [32] calculated using an analytical model that the torque will be always positive and a prolate spheroid will be always driven into alignment with the parallel electrodes if the gap size is larger than the length of the spheroid. The maximum dielectrophoretic torque was found for a tilt angle close to  $30^\circ$ . Nanowires longer than the distance between electrodes by two or more times were shown to be mis-oriented with respect to the microelectrode pair. These findings are in agreement with the achieved results, where several 30- $\mu\text{m}$ -long PZT microtubes are not well oriented across the electrode array with 12  $\mu\text{m}$  spacing.

The effect of a sinusoidal voltage on positioning and aligning of PZT tubes across the interdigitated electrode structure was found to be ineffective for the electric field amplitudes and frequencies in the range of 1-15  $V_{\text{rms}}$  and 10 Hz – 1 MHz, respectively, and needs to be further studied. Also, a design of more intricate

electrode structures providing spatially confined electric-field profile with greater alignment and capture forces is necessary.

## CONCLUSIONS

In summary, high aspect ratio ferroelectric tube structures made of PZT were successfully fabricated via template wetting technique. Using the repeated infiltration of a PZT liquid precursor into the pores of silicon templates under sub-atmospheric pressure, a uniform coating of the pore walls was achieved. On partial removal of the Si template, it was possible to produce a periodic array of free-standing ferroelectric tubes as mold replicas of a regular array of 2-D pores. The XRD and SEM analysis showed that thermal annealing at  $750^\circ\text{C}$  for 2 min in oxygen provides polycrystalline tubes of aspect ratio of about 20 with mainly perovskite structure. Therefore, the vacuum infiltration technique can be used as an alternative approach to other wafer-scale fabrication methods for producing ordered arrays of ferroelectric 1-D like structures as well as discrete microtubes with tailored dimensions.

The as-synthesized microtubes can be readily manipulated and so would facilitate the fabrication of more complicated structures for use in miniaturized electronic devices, including piezoelectric MEMS or NEMS actuators and sensors, and ferroelectric high-density FeRAM memories. To arrange tubes over large wafer areas, a simple and inexpensive method based on dielectrophoresis has been employed in the present work. The electric field-assisted assembly of PZT microtubes between the parallel electrodes would allow, in first step, for quick and simple creation of electrical connections at ambient conditions, and hence making a testing tube structure for rapid electrical characterization. Dielectrophoretic behavior study with different shapes, amplitudes and frequencies of the applied voltage revealed that a rectangular voltage of 5  $V_{\text{rms}}$  and 10 Hz is the most effective in assembling PZT microtubes between the electrodes with 12- $\mu\text{m}$  spacing. A frequency variation in the range of 1-10 Hz at fixed amplitude of the biasing voltage was found to improve the overall alignment of the tubes. These findings demonstrate that the dielectrophoretic technique has a great potential to control the alignment and placement of large numbers of PZT microtubes from solution onto pre-patterned electrodes using dielectrophoresis.

## Acknowledgements

*The support of this research by the Grant Agency of the Slovak Academy of Sciences through grant No 2/0053/11, the Slovak Research and Development*

Agency through grant No APVV-0222-10 and COST MP0904 Action is gratefully acknowledged. The author appreciates valuable discussions on the processing and assembly of ferroelectric microtubes with Professor Susan Trolier-McKinstry and Professor Theresa Mayer and wishes to thank Dr. S. Bharadwaja and Dr. M. Li for their technical assistance within a Fulbright Scholarship Grant No. G-1-00005 at the Pennsylvania State University.

## References

1. Scott J.F.: *Science* 315, 954 (2007).
2. Wang Z.L.: *Adv. Mat.* 19, 889 (2007).
3. Lieber C.M., Wang Z. L.: *MRS Bull.* 32, 99 (2007).
4. Bhat V.V., Madhusoodhana C.D., Umarji A.M.: *Ferroelectr.* 332, 97 (2006).
5. Naumov I.I., Bellaiche L., Fu H.: *Nature* 432, 737 (2004).
6. Robertson J.: *Mat. Today* 10, 36 (2007).
7. Morrison F.D., Ramsay L., Scott J.F.: *J. Phys.: Cond. Matt.* 15, L527 (2003).
8. Rørvik P.M., Tadanaga K., Tatsumisago M., Grande T., Einarsrud M.A.: *J. Eur. Ceram. Soc.* 29, 2575 (2009).
9. Luo Y., Szafraniak I., Zakharov N., Nagarajan N., Steinhart M., Wehrspohn R., Wendorff J.H., Ramesh R., Alexe M.: *Appl. Phys. Lett.* 83, 440 (2003).
10. Bharadwaja S.S.N., Olszta M., Trolier-McKinstry S., Li X., Mayer T., Roozeboom F.: *J. Am. Ceram. Soc.* 89, 2695 (2006).
11. Kim J., Yang S.A., Choi Y.Ch., Han J.K., Jeong K.O., Yun Y.J., Kim D.J., Yang S.M., Yoon D., Cheong H., Chang K.S., Noh T.W., Bu S.D.: *Nano Lett.* 8, 1813 (2008).
12. Bharadwaja S.S.N., Moses P.J., Trolier-McKinstry S., Mayer T.S., Bettotti P., Pavesi L.: *IEEE Trans. UFFC* 57, 792 (2010).
13. Wang M.C.P., Gates B.D.: *Mat. Today* 12, 34 (2009).
14. Pohl H.A.: *J. Appl. Phys.* 22, 869 (1951).
15. Pohl H.A.: *J. Appl. Phys.* 29, 1182 (1958).
16. Smith P.A., Nordquist Ch.D., Jackson T.N., Mayer T.S., Martin B.R., Mbindyo J., Mallouk T.E.: *Appl. Phys. Lett.* 77, 1399 (2000).
17. Krupke R., Hendrich F., Lohneysen H.V., Kappes M. M.: *Science* 301, 344 (2003).
18. Lee S.Y., Kim T.H., Suh D.I., Cho N.K., Seong H.K., Jung S.W., Choi H.J., Lee S.K.: *Chem. Phys. Lett.* 427, 107 (2006).
19. Lee S.Y., Umar A., Suh D.I., Park J.E., Hahn Y.B., Ahn J.Y., Lee S.K.: *Physica E* 40, 866 (2008).
20. Kumar S., Yoon S.H., Kim G.H.: *Curr. Appl. Phys.* 9, 101 (2009).
21. Jones T.B.: *Electromechanics of Particles*, Cambridge University Press, New York, 1995.
22. Wolf R.A., Trolier-McKinstry S.: *J. Appl. Phys.* 95, 1397 (2004).
23. Kwok C.K., Desu S.B.: *Appl. Phys. Lett.* 60, 1430 (1992).
24. Hamedi L.H., Guilloux-Viry M., Perrin A., Li Z.Z., Raffy H.: *J. Solid State Chem.* 158, 40 (2001).
25. Green N.G., Ramos A., Morgan H.: *J. Phys. D: Appl. Phys.* 33, 632 (2000).
26. Pohl H.A.: *Dielectrophoresis*, Cambridge University Press, Cambridge, 1978.
27. Aubry N., Singh P.: *Europhys. Lett.* 74, 623 (2006).
28. Liu Y., Chung J.H., Liu W.K., Ruoff R.S.: *J. Phys. Chem. B* 110, 14098 (2006).
29. Raychaudhuri S., Dayeh S.A., Wang D., Yu E.T.: *Nano Lett.* 9, 2260 (2009).
30. Dimaki M., Bøggild P.: *Nanotechnology* 15, 1 (2004).
31. Crews N., Darabi J., Voglewede P., Guo F., Bayoumi A.: *Sens. Actuators B* 125, 672 (2007).
32. Liu W.J., Zhang J., Wan L.J., Jiang K.W., Tao B.R., Li H.L., Gong W.L., Tang X.D.: *Sens. Actuators B* 133, 664 (2008).
33. Xu D., Subramanian A., Dong L., Nelson B.J.: *IEEE Trans. Nanotech.* 8, 449 (2009).
34. Jones T.B.: *IEEE Eng. Med. Biol. Mag.* 22, 33 (2003).